Jordan Journal of Civil Engineering, Volume **11**, No. **1**, **2017**

Predicting the Seismic Response of Structures Employing Controlled Rocking As a Form of Base Isolation

Omar Shamayleh

Engicon Consulting Engineers, Jordan. E-Mail: oshamayleh@engicon.com

ABSTRACT

A wide variety of rocking systems have been proposed to reduce damage induced by earthquakes. These systems rely on rocking as a form of base isolation, but also employ post-tensioning to limit rocking amplitude and ensure re-centering of the system. Often, performance-based design approaches (i.e., static pushover) are used to predict the response of these systems.

This paper employs a simple analytical model to investigate the response of post-tensioned flexible rocking structures using two different approaches. First, analytical dynamics approach is used to predict the full dynamic response. Second, a performance- based design approach is used to predict the maximum response. The simple model allows a wide parametric study to determine the effects of relative tendon stiffness, relative structural stiffness and rocking parameters, on the maximum response.

Comparison of the results defines limits for the relative tendon stiffness and the rocking amplitudes for which performance- based design approaches are reliable. Beyond these limits, the full dynamic response must be considered. In addition, the results give insight into the parameters for which the benefits of rocking behavior can best be exploited.

KEYWORDS: Rocking, Earthquake engineering, Seismic response, Base isolation, Perfromance-based design.

INTRODUCTION

The purpose of the current generation of seismic design provisions is to protect life safety by preventing building collapse. These traditional methodologies were not developed to prevent damage to buildings and infrastructure or mitigate economic losses.

Developing seismic provisions and codes enabling the design of structures to achieve defined seismic performance levels is a pressing requirement in mitigating future losses from earthquake hazards. In order to achieve performance levels higher than "life-safety", reliable retrofit and design techniques are required, enabling the isolation of structures from ground motion, reducing earthquake generated forces and, consequently, minimizing response, material strains and damage (ATC, 2006).

Rocking systems as a form of base isolation for bridge piers and building frames have been the subject of several recent studies. The first systematic investigation of the dynamics of rocking was conducted by Housner (1963), who examined the dynamic behaviour of a rigid rectangular slender block, resting on a level surface and rocking about its bottom corners under horizontal ground motion. Housner's investigation showed that tall, slender blocks are unexpectedly stable under earthquake excitation, more

Received on 9/4/2015.
Accepted for Publication on 31/5/2015.

than would be intuitively inferred by their stability against steady lateral loading. Subsequent studies have shown structures designed to uplift and rock on their foundations during earthquakes, experiencing significantly reduced deformations and consequently sustaining less damage than fixed-base counterparts. Subsequent investigations (Meek, 1975; Chopra and Yim, 1985; Psycharis, 1991) have shown a desirable base isolation effect resulting from foundation uplift in structures subjected to ground motion.

Oliveto et al. (2003) built upon these findings to derive the non-linear equations of motion for large displacements, enabling an investigation of the overturning stability of a single-degree-of-freedom flexible structure with foundation uplift, noting that a thorough understanding of the dynamic behaviour of rocking structures was still required. Acikgoz and DeJong (2012, 2013) further investigated the interaction of structural flexibility with base rocking for flexible rocking structures under pulse-type excitations, highlighting the effect of elasticity as dominant pulses in near field earthquake records, which are often responsible for the overturning collapse of rocking structures. These studies have made it feasible to develop a design methodology capable of accurately capturing the maximum response and hence enabling the design of configurations to meet specific performance requirements.

This cumulative work has shown that rocking can potentially be implemented as a form of base isolation to eliminate inelastic dynamic structural response. Further research has shown that controlled rocking enhances these effects, by limiting rocking amplitude and ensuring self-centering, virtually eliminating residual drifts and ensuring that the system remains essentially elastic (Eatherton et al., 2008).

An ongoing reappraisal of seismic design principles by the engineering community has resulted in a gradual realignment from force-based to performance-based seismic design. Performance objectives are increasingly employed to define the level of acceptable risk (Priestley, 2000).

Recent research has proposed applying current performance-based design approaches to controlled rocking systems. Pollino and Bruneau (2007) analytically investigated a seismic retrofit technique for steel truss bridge piers, featuring a rocking-dissipating pier-foundation connection. Pollino and Bruneau's proposed system features a passive energy dissipation device (buckling restrained brace) which enhances self-centering. Performance-based methods were used to predict maximum deck-level response (displacement), implementing the non-linear static coefficient-capacity spectrum procedure (FEMA, 1997).

However, fundamental differences in behaviour between rigid rocking systems and linear elastic oscillators have led to questioning of performance-based design approaches proposed to predict the response of such systems, almost all of which employ linear elastic displacement response spectra for demand estimation (Makris and Konstantinidis, 2003). Given the limitations of static analysis procedures (e.g., pushover analysis), the reliability of the maximum response predictions of controlled rocking structures using current methods has not been sufficiently investigated. In order to fully realize the potential of controlled rocking systems, further research is required to:

- Evaluate existing Performance-Based Design (PBD) methods as a viable seismic design approach.
- Define the limitations of Performance-Based Design (PBD) using static analysis techniques and identify design constraints necessary to achieve optimum benefits of rocking behaviour.
- Extend recent advances in the fundamental understanding of the interaction of flexibility and rocking in free-standing flexible rocking structures to controlled (post-tensioned) flexible rocking structures.

MODELLING AND ANALYSIS METHODS

A. Structural Model

An idealized model of the system under

consideration; a post-tensioned flexible rocking structure, is shown in Figure 1. The model has a lumped mass *m*, positioned at height *H* at quiescent initial conditions and attached to a weightless, rigid foundation beam of width *2B*, by an axially rigid strut of lateral stiffness k_o and viscous damping *c*. The diagonal distance from the undisturbed mass to points *O*,*O′* located at the edges of the base foundation, is denoted as $R_0 = \sqrt{(B^2 + H^2)}$ and $\alpha = tan^{-1}(B / H)$ is the angle of slenderness. A central, unbonded post-tensioned elastic tendon of stiffness k_t passes through a duct running through the center of the structure. The two - degree- of- freedom system is free to uplift and may respond to horizontal excitations by rocking about pivot points *O*,*O′* in addition to translational motion of the mass, *u*.

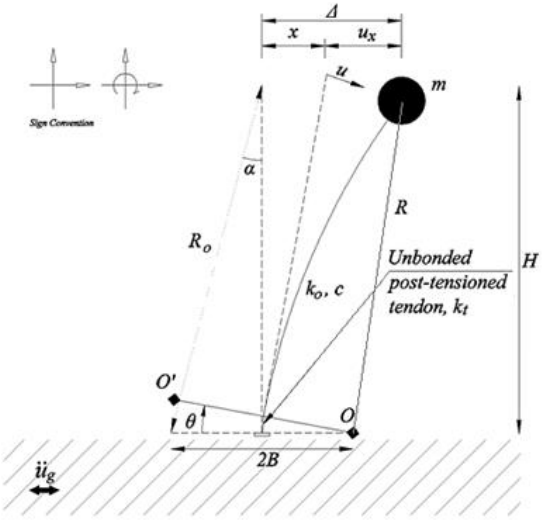

Figure (1): Schematic of idealized structural model of a post-tensioned, flexible rocking structure

Horizontal displacement $\Delta = x + u_x$, where *x* is the horizontal component of rocking displacement and u_x is the horizontal component of lateral deformation *u*.

$$u_x = u\cos(\theta) \quad (1)$$

$$x = R\sin(\alpha) - R\sin(\alpha - \theta). \quad (2)$$

The configuration shown in Figure 1, representing the system considered in this investigation, also represents common design and retrofit solutions used in practice. For the purposes of this study, analyses were conducted assuming that the system rests on rigid ground and that the coefficient of static friction is sufficient to prevent sliding. In practice, sliding may also be prevented by using an appropriate foundation configuration.

B. Phases and Associated Equations of Dynamic Motion

Two phases define the dynamic motion of a flexible rocking structure; a phase in full contact with the ground and an uplifted, rocking phase. The equations of motion governing these two states for a free-standing (no additional self-centering), flexible rocking structure are presented in (Acikgoz and DeJong, 2013).

In the current model, the equations of motion for the rocking phase account for the added post-tensioned tendon. The full contact phase is unaffected by this addition, as the tendon is not assumed to be prestressed; i.e., it is slack prior to uplift and only exerts a resorting force in the event of rocking. The equations of motion for the rocking phase are adopted from (Acikgoz and DeJong, 2013), expanding the model to include a post-tensioned tendon.

Full contact phase: This phase represents the response of a structure with quiescent initial conditions, such that both corners of the base are in contact with the ground. The structure's motion is identical to that of a linear elastic oscillator and is governed by the standard differential equation for a SDOF system:

$$\ddot{u} + 2\zeta\omega_n\dot{u} + \omega_n^2 u = -\ddot{u}_g; \quad (3)$$

where *u* is the elastic translation of the mass, $\omega_n = \sqrt{(k/m)}$ is the angular natural frequency of the system, $\zeta = c/(2\sqrt{km})$ is the damping factor and $\ddot{u}_g$ is the horizontal ground acceleration. The response of the structure in this phase is not affected by geometry, provided that stiffness *k* is an independent parameter.

Rocking phase: Once the structure uplifts, rocking and elastic deformation proceed simultaneously. This occurs once lateral displacement of the mass *m* reaches a critical value u_{cr} at which the overturning moments are sufficient to cause uplift. The equations of motion governing the rocking phase, which describe the elastic translation and rocking for a free rocking (unanchored) structure, were derived in (Acikgoz and DeJong, 2012) using generalized coordinates (R,β) and extended in (Acikgoz and DeJong, 2013) using (u,θ), based on a model formulated by Oliveto et al. (2003). The (u,θ) coordinates are used in this study exclusively and equations have been modified for a SDOF system. The equations of motion for the rocking phase in terms of these parameters are (variables given in Figure 1):

$$\ddot{u} + H\ddot{\theta} + (\pm B - u)\dot{\theta}^2 + 2\zeta\omega_n\dot{u} + {\omega_n}^2 u = -\ddot{u}_g\cos(\theta) + g\sin(\theta). \quad (4\text{ a})$$

$$(R_o^2 + u^2 \mp 2Bu)\ddot{\theta} + H\ddot{u} \mp 2\dot{\theta}\dot{u}\,(B \mp u) + (k_t B^2\sin(\theta)/m) = +\ddot{u}_g(-R_o\cos(\alpha \mp \theta) + u\sin(\theta)) + g(\mp R_o\sin(\alpha \mp \theta) + u\cos(\theta)). \quad (4\text{ b})$$

Equation (4 a) describes the rocking motion of a flexible rocking structure, retrofitted with an unbonded central tendon. The first line of this equation represents the equilibrium of forces in the direction of elastic deformation u, while the second line represents the equilibrium of overturning and stabilizing moments about the rocking pivot O (or O'). The term $(k_tB^2sin(\theta)/m)$ accounts for the elastic action of the tendon. In Equation (4 a), the upper sign indicates rotation about the right base corner O and the lower sign indicates rotation about the left foundation corner O'. Details of phase transition can be found in (Acikgoz and DeJong, 2012).

C. Performance-Based Design Approach

This section presents the analysis procedure and design requirements for performance-based seismic design of controlled rocking structures. The adopted analysis procedure is the Nonlinear Static Procedure (NSP), often referred to as the Pushover Analysis (PA) (FEMA, 1997; ATC, 1996). Under this procedure, a model directly incorporating non-linear response is displaced to a target displacement and the resulting forces are measured.

This procedure has been adopted from ATC-40 (ATC, 1996) and modified to account for bilinear elastic behaviour characteristics of controlled rocking structures. The original document refers to inelastic material response as the source of non-linearity. However, this was modified so that the limit state at which the system's stiffness deviates is the uplift of the structure, as opposed to gradual yielding of structural members.

A mathematical model of the structure is developed, in accordance with guidelines specified in ATC-40 (ATC, 1996). This model is subjected to monotonically increasing horizontal forces until a target displacement is achieved. Seismic demand can be directly expressed as elastic spectral demand. It is then possible to compare seismic demand with the structure's lateral force-displacement (pushover) capacity. This is the basis of Capacity Spectrum Method (CSM); a performance-based seismic design method described in the ATC-40 document (ATC, 1996).

D. Dimensionless System

To present the results in an intuitive manner, for a wide range of structures, input parameters are non-dimensionalized. Furthermore, in order to characterize the behaviour of the system, the absolute ratio of the rotational stiffness provided by the tendon to the rocking rotational stiffness is adopted.

Additional moment provided by the unbonded post-tensioned tendon has been shown to be:

$$M_{add,tendon} = k_t B^2 \sin\theta\,; \quad (5)$$

where k_t = tendon stiffness. Normalizing by moment of inertia of the mass and the frequency parameter:

$$I = mR^2, \qquad p = \sqrt{g/R}. \quad (6)$$

$$\frac{M_{ad}}{p^2 I} = \frac{k_t B^2 \sin\theta}{mgR}. \quad (7)$$

Assuming small angle rotation, applying the elastic moment rotation relationship:

$$M = k\theta. \quad (8)$$

$$\frac{M_{ad}}{p^2 I} = \frac{k_t B^2 \sin\theta}{mgR} \approx \frac{k_t B^2 \theta}{mgR} = \rho_t \theta. \quad (9)$$

$$\rho_t = \frac{k_t B^2}{mgR}, \qquad k_t = \frac{\rho_t mgR}{B^2}. \quad (10)$$

A characterization of systems retrofitted with three ranges of rotational stiffness can be achieved using the dimensionless quantity ρ_t. Varying the values of ρ_t, its value will allow for capturing these three ranges of rocking behaviour.

$$\left|\frac{M_{ad}}{M_{gr}}\right| = \left|\frac{K_{R,ad}}{K_{R,gr}}\right| = \boldsymbol{\rho_t} = \begin{cases} \to 0 \ rocking\ system & \text{(negative slope)} \\ = 1 \ balanced\ system & \text{(zero slope)} \\ \gg 1 \ hybrid\ system & \text{(posotive slope)} \end{cases} \quad (11)$$

Use of this parameter facilitates the determination of the effects of relative tendon stiffness on maximum response.

A flexibility/scale non-dimensional parameter ρ_o will be used to determine and capture the effects of relative structural (bending) stiffness.

$$\rho_o = \frac{k_o B^2}{mgR} = \frac{\omega_n{}^2 B^2}{p^2 R^2}. \quad (12)$$

$$\frac{\omega_n}{p} = \sqrt{\rho_o}\frac{B}{R}. \quad (13)$$

The behaviour of the system will depend on the dimensionless terms $\theta/\alpha, u/u_{cr}$, ρ_o, ρ_t, but will also be determined by the characteristics of the specific ground motion records to be implemented. In that sense, the response is not completely non-dimensionalized. However, response can be presented intuitively in terms of $\theta/\alpha, u/u_{cr}$, and compared across the range of ground motions implemented, for a wide range of relative structural stiffness and relative tendon stiffness ρ_o, ρ_t, representing a variety of behaviours which can be captured using these parameters.

ANALYSIS AND RESULTS

The viability of the proposed model is assessed by means of a case study. A bridge pier configuration with geometrical and material properties consistent with an existing structure is introduced in this section. A detailed example illustrates how results are obtained and compared in a parametric study.

The performance-based procedure applied in the current research, the capacity spectrum method (ATC, 1996), will be explained using an example. The case study is a precast concrete bridge pier configuration with geometrical and material properties consistent with an existent bridge, the South Rangitikei Rail Bridge in New Zealand, which by design employs rocking as a seismic isolation technique (Ma and Khan, 2008). This configuration is modified for the purposes of this study by the addition of a central unbonded post-tensioned tendon as a self-centering device. The height of the pier H = 76.9 m, half base width B = 6.73 m and mass m=1.67×10^6 kg lumped at deck level, assumed to be at height H. The pier's aspect ratio is 11.5, corresponding to a slenderness angle α=0.09 rad. The pier is allowed to uplift and rock on its foundation under the influence of horizontal ground motion. Sliding is assumed to be prevented by means of an appropriate foundation configuration.

A. Design Example

The bridge is assumed to be located at class B, representing a rock site and coefficients F_a and F_v = 1. A site-specific design response spectrum, calculated according to procedures described in the Guidelines for the Seismic Design of Highway Bridges (AASHTO, 2007), based on 5% in 50 year probabilistic data from the US geological survey (USGS, 2013), is used to obtain seismic demand. One-second (S_1) and short period (Ss) acceleration values are 0.734g and 1.93g, respectively, corresponding to 5% damping.

Values of relative stiffness parameters ρ_o, ρ_t, correspond to stiffness categories, representing proportional multiples of absolute lateral and relative

stiffness, respectively, according to (Eq. 10 and Eq. 12). Tendon stiffness k_t is considered in multiples of 28000 kN/m, which corresponds to a relative tendon stiffness of ρ_t=1 and represents the tendon stiffness required to balance the pier's negative 'rocking stiffness' for small rotations, resulting in a horizontal post-uplift stiffness curve.

Thus, for (ρ_t =1)→k_t=28×10^3 kN⁄m (Eq. 10). The pier's lateral stiffness k_o is similarly considered in multiples of 28×10^3 kN⁄m, which corresponds to a relative initial stiffness of (ρ_o =1), as defined in Eq. 12.

Horizontal deck-level displacement for selected values of ρ_o, ρ_t is shown in Figure 2. The values of ρ_o, ρ_t this example uses are used to obtain values of k_o,k_t. (Eq. 10 and Eq. 12). These stiffness values determine the shape of the bilinear elastic force displacement curve to be employed in the pushover analysis.

Taking ρ_o = *5*, ρ_t= *100* as an example case:

$$k_o = \frac{\rho_o mgR}{B^2} \rightarrow \rho_o = 5 \rightarrow k_0 = 141 \times 10^3\ kN/m;$$

$$k_t = \frac{\rho_t mgR}{B^2} \rightarrow \rho_t = 100 \rightarrow k_t = 28 \times 10^5\ kN/m.$$

B. Non-linear Inelastic Time History Analysis

In order to verify the effectiveness of the performance-based approach employed herein, a non-linear dynamic time-history analysis is performed to predict the full 'exact' dynamic response. For the analytical dynamics simulation, the absolute stiffness values are determined from relative stiffness values ρ_o, ρ_t (Eq. 10 and Eq. 12). These absolute stiffness values (in units of kN⁄m), pier mass m and dimensions H, B constitute input parameters for the numerical solution of the equations of motion (Eq. 3 and Eq. 4). The result of this simulation can be expressed in terms of the non-dimensional output parameters θ/α,u/u_{cr} or directly as the total deck-level lateral displacement Δ which is evaluated according to Eq.1.

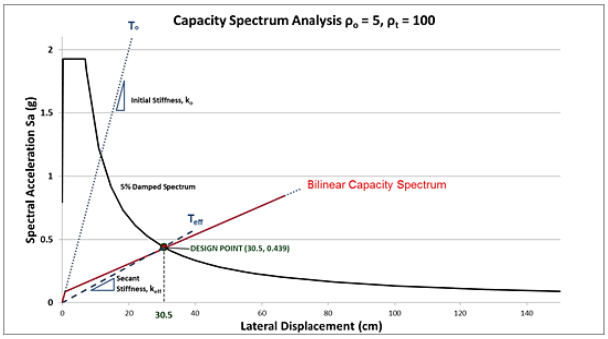

Figure (2): Example capacity spectrum analysis (ATC, 1996)

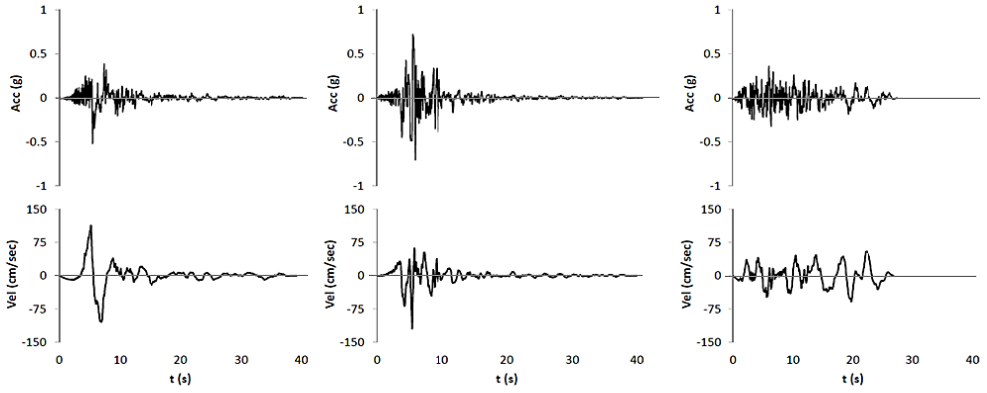

(a) (b) (c)

Figure (3): Pulse type ground motion records (a) 1979 Imperial Valley (El Centro Array #4) [IV79] and (b) 1994 Northridge (Newhall, Fire Station) [NR94] and non-pulse-type record (c) 1980 Victoria Mexico (Chihuahua) [VM80]. Acceleration time histories of the selected records are shown in the top row and velocity time histories are shown in the bottom row (Pacific Earthquake Engineering Research Center, 1014)

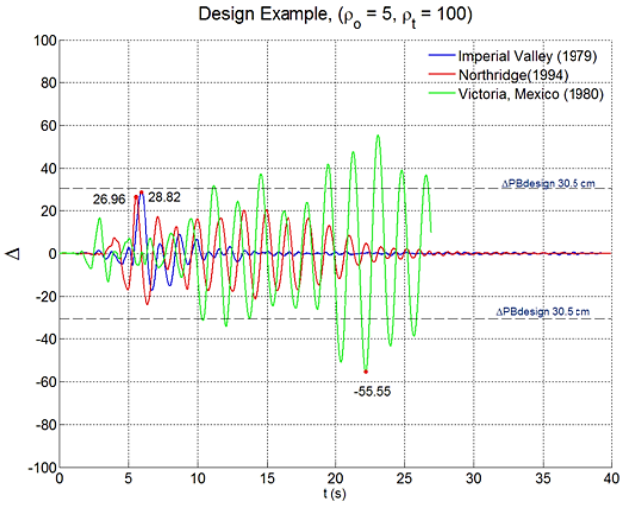

Figure (4): Lateral pier displacement Δ results of example time history analysis

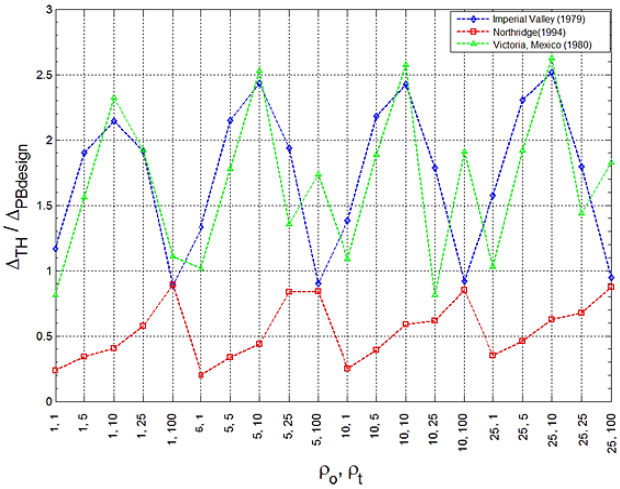

Figure (5): Non-linear time-history simulation results for deck-level displacements Δ, normalized by their respective displacement-based design response value

Previous research into performance-based design of controlled rocking systems, e.g. (Pollino and Bruneau, 2007), used synthetic earthquake records lacking "forward directivity effects in the near fault region" characteristics (Baker, 2007). Specifically strong velocity pulses caused by fault normal, near fault pulse-type ground motion are the primary drivers of large amplitude rocking (Housner, 1963; Acikgoz and DeJong, 2013). In the current research, viability of the proposed model is assessed by subjecting the bridge pier configuration to both pulse type and non-pulse type earthquake records. Time-history plots of the ground motion records used in this study are shown in Figure 3. The records were obtained from the PEER ground motion database (PEERC, 2014).

Comparison of Results of Maximum Deck-Level

Displacement predictions by the performance-based method and the full dynamic time-history analysis are presented as maximum response predicted by the time-history analysis ΔTH shown in Figure 4 normalized by the maximum response predicted by the performance-based design procedure ΔPB design shown in Figure 2.

C. Paramteric Study

A parametric study using analytical dynamics (non-linear time-history analysis) is conducted to determine the accuracy of maximum response values predicted by the displacement-based procedure used in this study, the Capacity Spectrum Method (ATC, 1996). As illustrated in the case study presented in the previous section, the primary parameters considered are relative tendon stiffness and relative structural stiffness ρ_o, ρ_t. Rocking parameters are also considered here with further recommendations for future work. A wide range of relative structural tendon stiffness is considered to determine the effects of these parameters on maximum response and the limits for which performance-based design approaches are reliable. The preliminary results of this parametric study are shown in Figure 5.

DISCUSSION

As shown in Figure 5, the displacement-based method conservatively predicts the maximum displacement for the 1994 Northridge ground motion for all twenty cases considered. Within each relative bending stiffness category, ρ_o, the performance-based approach is seen to more accurately predict maximum response for higher values of ρ_t, representing a stiffer

tendon. Conversely, for the 1979 Imperial Valley ground motion, the performance-based approach under-predicts response for all but four cases. These four cases, which are slightly over-predicted, pertain to the stiffest tendon, ρ_t =100 for all bending stiffness categories, ρ_o =1, 5, 10 and 100. Prediction of maximum displacement is unconservative for all but two cases for the 1980 Victoria, Mexico ground motion.

A monotonic, upward trend in displacement-based method predictions is noticeable for the 1994 Northridge ground motion, such that predictions for lower relative tendon stiffness ρ_o values are very conservative, but the accuracy of prediction gradually increases with increasing tendon stiffness until a very good prediction is realized at ρ_t =100, a case which represents the highest relative tendon stiffness. This pattern is similarly observed for higher bending stiffness categories ρ_o =5, 10 and 25.

For the 1979 Imperial Valley ground motion, the displacement-based method also yields predictions of noticeable variation within structural stiffness categories. The pattern of variation is then approximately repeated across bending stiffness categories; i.e., for ρ_o =1,5,10 and 25. However, in this case, change in prediction accuracy is not monotonous within structural stiffness categories, as is the case for the 1994 Northridge ground motion. Rather, predictions are more accurate for very stiff and very flexible tendons ρ_t=100 and 1, respectively. Predictions are unconservative for three intermediate relative tendon stiffness categories ρ_t = 5, 10 and 25, with the least conservative prediction achieved at ρ_t =10.

Interestingly, the displacement-based method's prediction of maximum response for the 1979 Imperial Valley ground motion is most accurate for ρ_t=100 and almost identical to the prediction for another pulse-type ground motion, the 1994 Northridge earthquake record. In both cases, response is slightly over-predicted. This indicates that record-to-record variability is minimal when relative rotational stiffness is at its highest value. This may imply that limiting rocking amplitude by applying a stiff tendon could limit record-to-record variability. This can be verified by comparison of results with the third ground motion record and examining rocking amplitude time-histories.

Predictions of maximum response for the 1980 Victoria, Mexico ground motion are more chaotic, displaying less regular distribution of normalized response than the previous two ground motion cases. Some agreement can be seen for the lowest relative rotational stiffness category ρ_t =1. As for IV79, prediction discrepancy increases for stiffer tendons represented by ρ_t =5 and 10. At higher relative tendon stiffness, there is little order to discern from the normalized displacements. Examining response time-histories and amplitude time-histories is required for further interpretation.

CONCLUSIONS

The current study investigated the viability of applying performance-based design approach to rocking structures. This was conducted by assessing the capability of an established displacement-based design method to predict the response of structural systems adopting controlled rocking to limit damage due to earthquake-induced ground motion. Initial results show that for large bridge piers, long duration velocity pulses cause large rocking amplitudes that the performance-based method is unable to accurately predict.

The results that have been achieved so far and conclusions based on them represent initial results from a preliminary investigation. Three earthquake records were selected for investigation and applied to a single pier configuration. The current model needs to be further developed to account for hysteric and radiation damping. A significant expansion of the number and type of earthquake ground motions, as well as the scale of structure considered, in addition to a suitable treatment of damping are required before generalizing results.

REFERENCES

AASHTO. (2007). "Guidelines for the seismic design of highway bridges". American Association of State Highway and Transportation Officials.

Acikgoz, M., and DeJong, M. (2012). "The interaction of elasticity and rocking in flexible structures allowed to uplift". doi:10.1002/eqe.

Acikgoz, M., and DeJong, M. (2013). "Analytical and experimental observations on vibration modes of flexible rocking structures". In: Society for Earthquake and Civil Engineering Dynamics Young Engineers Conference - 2013 (1, 1–7). Newcastle.

ATC. (1996). "ATC-40 seismic evaluation and retrofit of concrete buildings (Vol. 1)". Federal Emergency Management Agency, Redwood City, California.

ATC. (2006). "FEMA 445 Next-generation performance-based seismic design guidelines program plan for new and existing buildings". Federal Emergency Management Agency, Redwood City, California.

Baker, J.W. (2007). "Quantitative classification of near-fault ground motions using wavelet analysis". Bulletin of the Seismological Society of America, 97, 1486-1501.

Chopra, A.K., and Yim, S.C.S. (1985). "Simplified earthquake analysis of multi-storey structures with foundation uplift". Journal of Structural Engineering, 111(12), 2708-2731. doi:10.1061/(ASCE)0733-9445(1985)111:12(2708).

Eatherton, M.R., Hajjar, J.F., Deierlein, G.G., Krawinkler, H., Billington, S., and Ma, X. (2008). "Controlled rocking of steel-framed buildings with replaceable energy-dissipating fuses". In: The 14th World Conference on Earthquake Engineering. Beijing, China.

FEMA. (1997). "NEHRP guidelines for the seismic rehabilitation of buildings". Federal Emergency Management Agency, Redwood City, California.

Housner, G.W. (1963). "Behaviour of inverted pendulum structures during earthquakes". Bulletin of the Seismological Society of America, 52 (2), 403-417.

Ma, Q.T., and Khan, M.H. (2008). "Free vibration test of a scale model of the South Rangitikei Railway Bridge". Proceedings of the New Zealand Society for Earthquake Engineering Annual Conference. Wairakei, New Zealand.

Makris, N., and Konstantinidis, D. (2003). "The rocking spectrum and the limitations of practical design methodologies". Earthquake Engineering and Structural Dynamics, 32 (2), 265-289. doi:10.1002/eqe.223

Meek, J. W. (1975). "Effects of foundation tipping on dynamic response". Journal of the Structural Division, 101 (7), 1297-1311.

Oliveto, G., Calio, I., and Greco, A. (2003). "Large displacement behaviour of a structural model with foundation uplift under impulsive and earthquake excitations". Earthquake Engineering and Structural Dynamics, 32 (3), 369-393. doi:10.1002/eqe.229.

Pacific Earthquake Engineering Research Center. (2014). "Ground motion database". Retrieved on March 10, 2014, from http://peer.berkeley.edu/.

Pollino, M., and Bruneau, M. (2007). "Seismic retrofit of bridge steel truss piers using a controlled rocking approach".

Priestley, M.J.N. (2000). "Performance-based seismic design". In: 12th World Conference on Earthquake Engineering (1, 1-22). Auckland, New Zealand.

Psycharis, I. N. (1991). "Effect of base excitation on dynamic response of SDOF structures". Journal of Structural Engineering, 117 (3), 733-754.

USGS. (2013). "Seismic hazard analysis tools". Earthquake Hazards Program. Retrieved on March 01, 2013, from http://earthquake.usgs.gov/.